KRITTIKA SUMMER PROJECTS 2024

# Study of Nearest Hydrogen-Rich Core-Collapse Supernova

Gaurav Bhoir

KRITTIKA SUMMER PROJECTS 2024
# Study of Nearest Hydrogen-Rich Core-Collapse Supernova

Gaurav Bhoir[1]

[1]St. Xavier's College

# Abstract

This project focuses on the detailed study of the nearest hydrogen-rich core-collapse supernova, SN2023ixf. Our investigation encompassed several key aspects, including image reduction, astrometry, and photometry, to analyze the supernova's properties accurately. We performed photometric analysis across multiple bands, with particular attention to the U-band, which presents additional challenges due to its sensitivity and atmospheric effects. Utilizing the luminosity model, we further explored the supernova's physical parameters, estimating the mass of the ejecta and the explosion energy. Our findings provide valuable insights into the nature of core-collapse supernovae, contributing to the broader understanding of stellar evolution and explosive nucleosynthesis.

# Contents

# 1. Introduction

Supernovae are among the most energetic and luminous events in the universe(1), marking the explosive death of certain types of stars. These cataclysmic events play a crucial role in the cosmic cycle of matter, dispersing heavy elements into space and triggering the formation of new stars. The type of supernova that occurs depends on the mass of the progenitor star and the specific conditions leading to the explosion.

## 1.1 Classification of Supernovae

Supernovae are classified based on their spectral characteristics and progenitor systems. The main types are:

### 1.1.1 Type I Supernovae

Type I supernovae are characterized by the absence of hydrogen lines in their spectra. They are further divided into subtypes:

- **Type Ia Supernovae**
  - **Progenitor**: A white dwarf in a binary system accretes material from a companion star until it reaches the Chandrasekhar limit and undergoes a thermonuclear explosion.
  - **Features**: Absence of hydrogen lines, presence of silicon absorption lines around maximum light. Light curves are generally symmetric with a well-defined peak.
- **Type Ib Supernovae**
  - **Progenitor**: Massive stars that have lost their outer hydrogen layers, typically through strong stellar winds or interactions with a companion star.
  - **Features**: Absence of hydrogen lines, presence of helium lines in the spectrum. Light curves are often asymmetrical.
- **Type Ic Supernovae**
  - **Progenitor**: Similar to Type Ib but with even more extensive loss of outer layers, including both hydrogen and helium.
  - **Features**: No hydrogen or helium lines, presence of silicon and iron lines. Often associated with gamma-ray bursts.

### 1.1.2 Type II Supernovae

Type II supernovae exhibit prominent hydrogen lines in their spectra and are typically the result of the core-collapse of massive stars. They are further divided into subtypes:

- **Type IIP (Plateau)**
  - **Progenitor**: Massive stars with a thick hydrogen envelope. These stars undergo core-collapse, resulting in a supernova with a plateau in the light curve.
  - **Features**: Long-lasting plateau in the light curve after the initial peak, strong hydrogen lines.
- **Type IIL (Linear)**
  - **Progenitor**: Similar to Type IIP but without the plateau phase in the light curve. The light curve shows a linear decline after the peak.
  - **Features**: Hydrogen lines are present, but light curve drops more steadily.
- **Type IIb**

- **Progenitor**: Massive stars that have lost most of their hydrogen envelope but still retain some.
        - **Features**: Evolving spectrum with strong hydrogen lines at early phases that later weaken, revealing helium and other elements.
  - **Type IIn**
    - **Progenitor**: Massive stars that explode in a dense circumstellar environment, often resulting from massive mass loss.
    - **Features**: Narrow hydrogen emission lines, with strong interaction features in the spectrum due to interaction with the circumstellar material.
  - **Type II-L**
    - **Progenitor**: Massive stars with a thinner hydrogen envelope.
    - **Features**: Linear decline in light curve without a plateau.
    - **Notable Example: SN 1987A**
      * **Discovery**: SN 1987A was observed in the Large Magellanic Cloud on February 23, 1987.
      * **Features**: Exhibits a complex light curve with a prominent early peak followed by a linear decline, strong hydrogen lines, and significant emission in the UV and optical bands.
      * **Importance**: SN 1987A is one of the closest supernovae observed in the modern era, providing invaluable insights into the mechanics of core-collapse supernovae and the stellar environments of massive stars.

### 1.1.3 Other Types

- **Type Ib/c Supernovae associated with Gamma-Ray Bursts (GRBs)**
    - **Progenitor**: Massive stars in a highly energetic state.
    - **Features**: Associated with long-duration GRBs and show evidence of high energy processes.
- **Type Ia Supernovae as Standard Candles**
    - **Application**: Used for cosmological measurements to determine the expansion rate of the universe.

## 1.2 About SN2023ixf:

### 1.2.1 Discovery

SN2023ixf is a Type II supernova discovered on May 19, 2023, by the amateur astronomer Koichi Itagaki. It was found in the spiral galaxy M101, also known as the Pinwheel Galaxy, located approximately 21 million light-years away from Earth in the constellation Ursa Major. The discovery was made through visual observations and confirmed by subsequent photometric and spectroscopic data.

### 1.2.2 Supernova Type

SN2023ixf is classified as a Type II-L supernova (5). Type II supernovae are characterized by the presence of hydrogen lines in their spectra, indicating that the progenitor star had a substantial hydrogen envelope prior to its explosion.

### 1.2.3 Progenitor Star

The progenitor star of SN2023ixf was likely a massive star with a significant hydrogen envelope (17). Such stars are generally red or blue supergiants, depending on their evolutionary stage at the time of the explosion. Although the specific characteristics of SN2023ixf's progenitor star are still under study, it is expected to have been a massive star with a mass in the range of 8 to 25 solar masses.

### 1.2.4 Light Curve and Spectrum

The light curve of SN2023ixf displays the typical features of a Type II-L supernova, including a prominent peak followed by a gradual decline. This variation over time provides insights into the explosion dynamics and the interaction of the ejecta with the surrounding medium. The spectrum of SN2023ixf shows strong hydrogen lines (13). Spectroscopic observations offer detailed information about the elements synthesized during the explosion and the physical conditions of the expanding supernova envelope.

## 1.3 Key Observations

### 1.3.1 Photometry

Observations in various photometric bands help determine the brightness and color evolution of SN2023ixf. This data is crucial for estimating the explosion's parameters, such as the total energy and mass of the ejected material.

### 1.3.2 Spectroscopy

Spectroscopic observations provide detailed information about the chemical composition of the supernova's ejecta and the velocity of the expanding material.

### 1.3.3 Scientific Significance

SN2023ixf plays a crucial role in understanding the mechanisms of core-collapse supernovae and the processes occurring during the final stages of massive star evolution. Studying SN2023ixf allows astronomers to gain insights into progenitor systems, explosion dynamics, and the synthesis of heavy elements.

## 1.4 Additional Observations

### 1.4.1 Distance and Host Galaxy

M101, the host galaxy, is a well-studied galaxy that provides context for understanding the environment in which SN2023ixf occurred. The distance to M101 is essential for calibrating the supernova's luminosity and other physical parameters.

This project involves a comprehensive study of SN2023ixf, focusing on image reduction, astrometry, and photometry. Special attention is given to U-band photometry, which is particularly challenging due to its sensitivity to atmospheric effects. By applying a luminosity model to the observed data, we estimate the mass of the ejecta and the explosion energy, providing insights into the physical properties of

the progenitor star. We will be trying to reproduce some of the data from (15) such as photometric modeling.

# Part One

# 2. Image Reduction



IMAGE PROCESSING

In this chapter, we describe the data reduction process undertaken for analyzing the supernova SN2023ixf. The raw data consisted of multiple FITS files, including science frames, bias frames, and flat frames. These images were processed using standard image reduction techniques to remove instrumental and atmospheric effects (0).

## 2.1  Introduction to Image Reduction

Image reduction is a crucial process in astronomical data analysis, where raw images captured by a CCD (Charge-Coupled Device) are processed to remove instrumental and environmental noise. This process enhances the quality of the data, allowing for more accurate scientific measurements. The main steps in image reduction include bias subtraction, flat-field correction, and dark current subtraction.
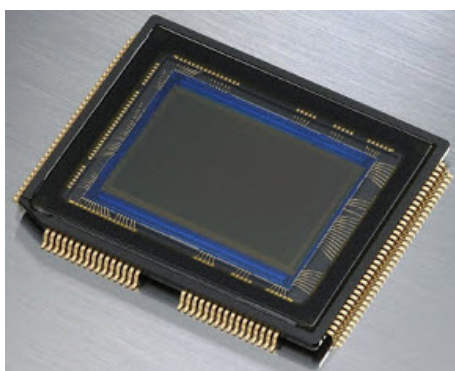


Figure 2.1: CCD

## 2.2  Charge-Coupled Devices (CCDs) and Image Formation

A Charge-Coupled Device (CCD) is a highly sensitive detector commonly used in astronomy to capture images of celestial objects. A CCD consists of an array of light-sensitive elements, called pixels, which convert incoming photons into an electric charge. The amount of charge collected by each pixel is proportional to the intensity of the light falling on it, thus creating an image.
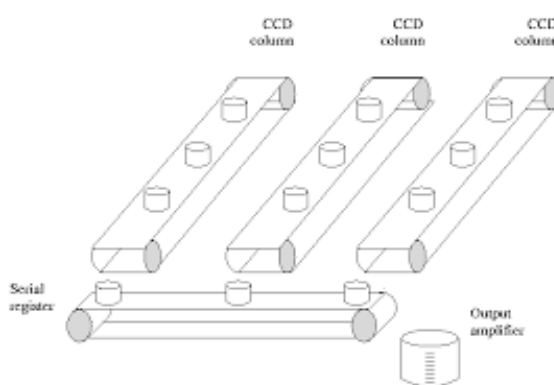


Figure 2.2: CCD pixel transfer

The image produced by a CCD is a two-dimensional array of pixel values, representing the intensity of light at different points in the field of view. However, the raw image is often contaminated with various types of noise and artifacts that must be removed before scientific analysis.

## 2.3 Growth India Telescope (GIT)

The Growth India Telescope (GIT) is a 0.7m fully robotic optical telescope located at the Indian Astronomical Observatory (IAO), Hanle, Ladakh. It is a collaborative project between the Indian Institute of Astrophysics (IIA), Bangalore, and the Inter-University Centre for Astronomy and Astrophysics (IUCAA), Pune. The primary aim of GIT is to conduct follow-up observations of transient events such as supernovae, gamma-ray bursts, and gravitational wave sources, making it a significant asset for time-domain astronomy.

GIT is an important tool for the Indian astronomical community, especially for the study of transients and variable stars. The telescope is also involved in multi-wavelength campaigns with other international observatories, enhancing its scientific output.



Figure 2.3: Growth India Telescope (GIT) at IAO, Hanle.

### 2.3.1 Specifications

The GIT has the following specifications:
- **Telescope:**
  - Aperture: 0.7m
  - Focal Ratio: F/6.5
  - Mounting: Altitude-Azimuth
- **CCD:**
  - Thermoelectric Cooling
  - Peak Quantum Efficiency: $> 95\%$
  - Read Noise: 8 electrons
  - Gain: 1.65 electrons/ADU
  - Linearity: Better than 99%
  - Optical Pixel Scale: $0.676 \times 0.676$ arcsec
  - Optical Field of View: $2769 \times 2777$ arcsec

- **Filters:**
    - Sloan Digital Sky Survey ugriz filters with 100nm broadband

The GIT's CCD camera has a high peak quantum efficiency of over 95%, making it very effective for detecting faint astronomical objects. The low read noise and high linearity ensure that the data quality is maintained across various observational conditions. The telescope's field of view, combined with its pixel scale, allows for detailed imaging of large sky areas, making it ideal for surveys and transient follow-up observations.

### 2.3.2 Significance of GIT

GIT plays a crucial role in the field of time-domain astronomy. With its automated scheduling and remote operation capabilities, it is well-suited for monitoring transient events that require immediate observation. Its contribution to the global network of observatories tracking transient phenomena is invaluable, providing data that is often used in conjunction with space-based telescopes and other ground-based facilities.

The data gathered by GIT has been instrumental in studying supernovae, variable stars, and other astrophysical phenomena. Its ability to perform rapid follow-up observations has led to significant discoveries and contributed to the understanding of the dynamic universe.

(**rao2018git**, **naik2019git**)

## 2.4 Bias Subtraction

The first step in the reduction process involved bias subtraction:

- We created a **master bias frame** by taking the median of multiple bias frames.
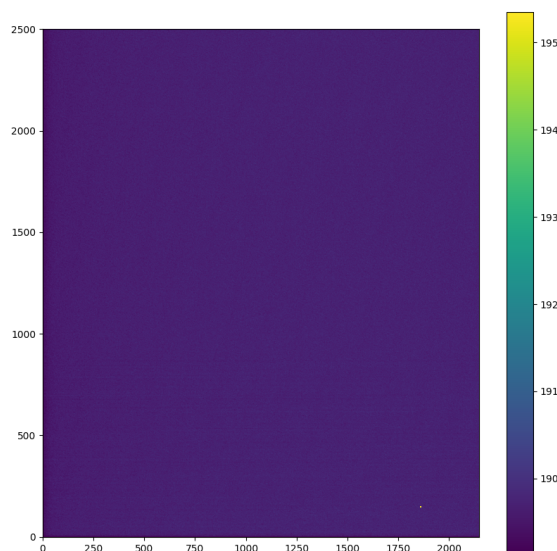


Figure 2.4: Bias file

- The master bias was then subtracted from all science and flat frames to correct for the electronic noise inherent in the CCD detector.
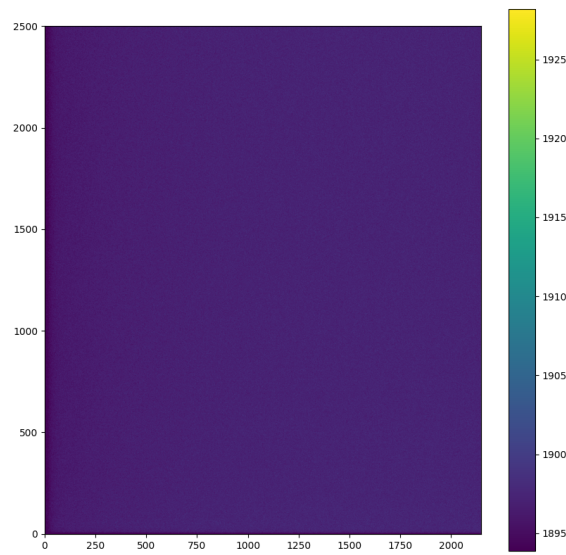
Figure 2.5: Master bias file

## 2.5 Flat Fielding

Next, we performed flat fielding to correct for pixel-to-pixel variations in sensitivity:
- A **master flat frame** was generated by taking the median of the flat frames.
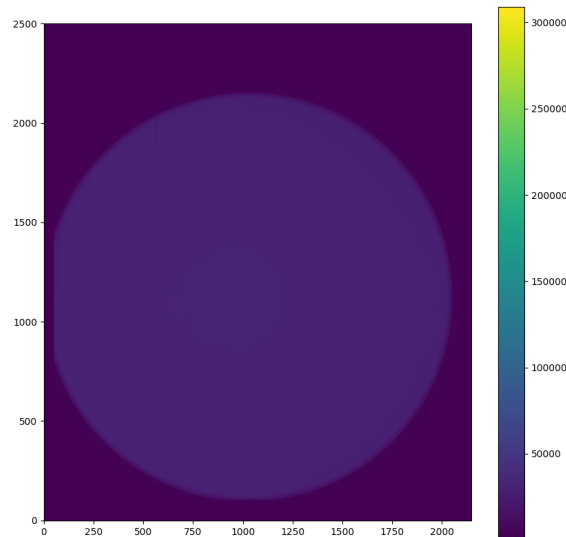


Figure 2.6: Flat file

- The master flat was then normalized.
- We divided the science frames by the normalized master flat to correct
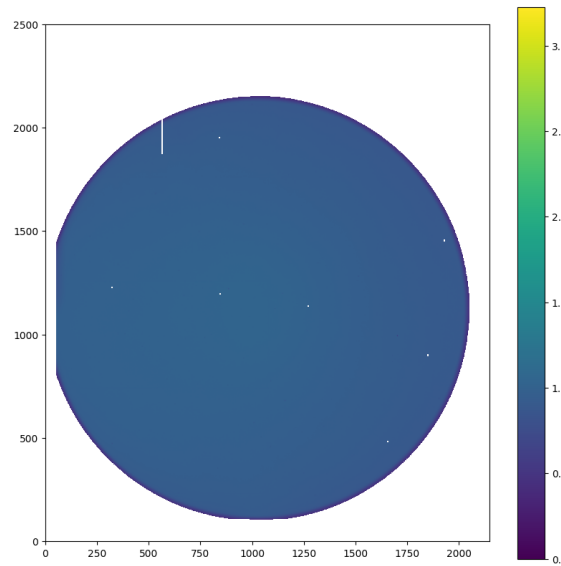
Figure 2.7: Master Flat file

## 2.6  Image Alignment and Stacking

After flat fielding, we aligned and stacked the images:
- The reduced science frames were aligned to correct for any shifts due to the telescope's tracking errors.
- The aligned frames were then stacked to improve the signal-to-noise ratio, resulting in a clearer analysis of SN2023ixf.
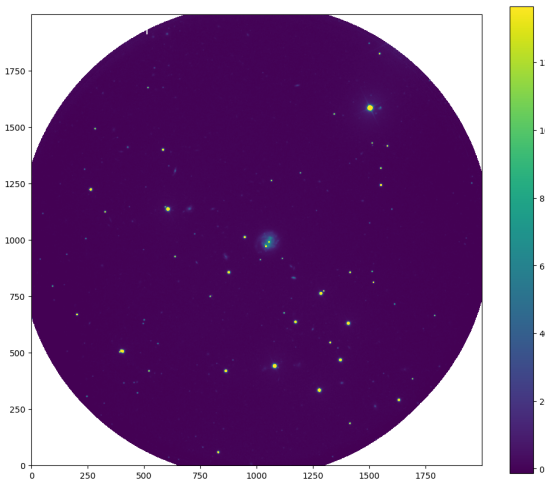


Figure 2.8:  All reduced images

This data reduction process prepared the FITS files for the subsequent phases of analysis, such as astrometry and photometry, ensuring that the frames were clean and properly calibrated.

# 3. Astrometry

## 3.1 Introduction to Astrometry

Astrometry is the branch of astronomy that deals with the precise measurement of the positions and movements of celestial objects. It is fundamental to many aspects of astrophysics, including the determination of stellar distances, the proper motion of stars, and the orbits of planets and other bodies within our solar system. Accurate astrometric measurements are essential for creating celestial reference frames, which are used for navigation and for measuring parallax to determine the distances to nearby stars (0).

Astrometry involves measuring the positions of stars and other celestial objects on the celestial sphere. These measurements are typically made using CCD images taken with telescopes. The key astrometric parameters include the object's position (right ascension and declination), proper motion (the rate at which an object moves across the sky), and parallax (the apparent shift in an object's position due to the Earth's motion around the Sun).

## 3.2 Astrometry Process

The process of astrometry involves the following steps:

1. **Image Acquisition:** High-quality images of the night sky are captured using a telescope equipped with a CCD camera. These images contain multiple celestial objects, including stars whose positions are to be measured.
2. **Image Calibration:** The images are corrected for various instrumental and atmospheric effects, such as bias, dark current, and flat-fielding, to ensure that the measurements are accurate.
3. **Star Detection and Centroiding:** The positions of stars in the images are determined by identifying the centroids of the star images, which correspond to the brightest pixels. This step is crucial as it defines the precise location of the stars in the image.
4. **Coordinate Transformation:** The pixel coordinates of the stars are converted into celestial coordinates (right ascension and declination) using a reference star catalog. This step often involves a plate solution, where the image is matched to known star positions from a catalog to determine the transformation between pixel coordinates and celestial coordinates.
5. **Error Analysis:** The uncertainties in the astrometric measurements are quantified, taking into account factors such as atmospheric turbulence, instrumental noise, and errors in the star catalog.

## 3.3 Astrometry for Our Project

In our project, we performed astrometry using Python to process the raw data and identify the positions of celestial objects. Python libraries such as `astropy` and `astroquery` were employed to handle the data and perform initial astrometric calculations.

After obtaining the initial results, we utilized the Aperture Photometry Tool (APT), an external software, to refine our astrometric measurements. APT provides a user-friendly interface for performing precise aperture photometry and astrometry, allowing us to accurately determine the positions of stars in our images.
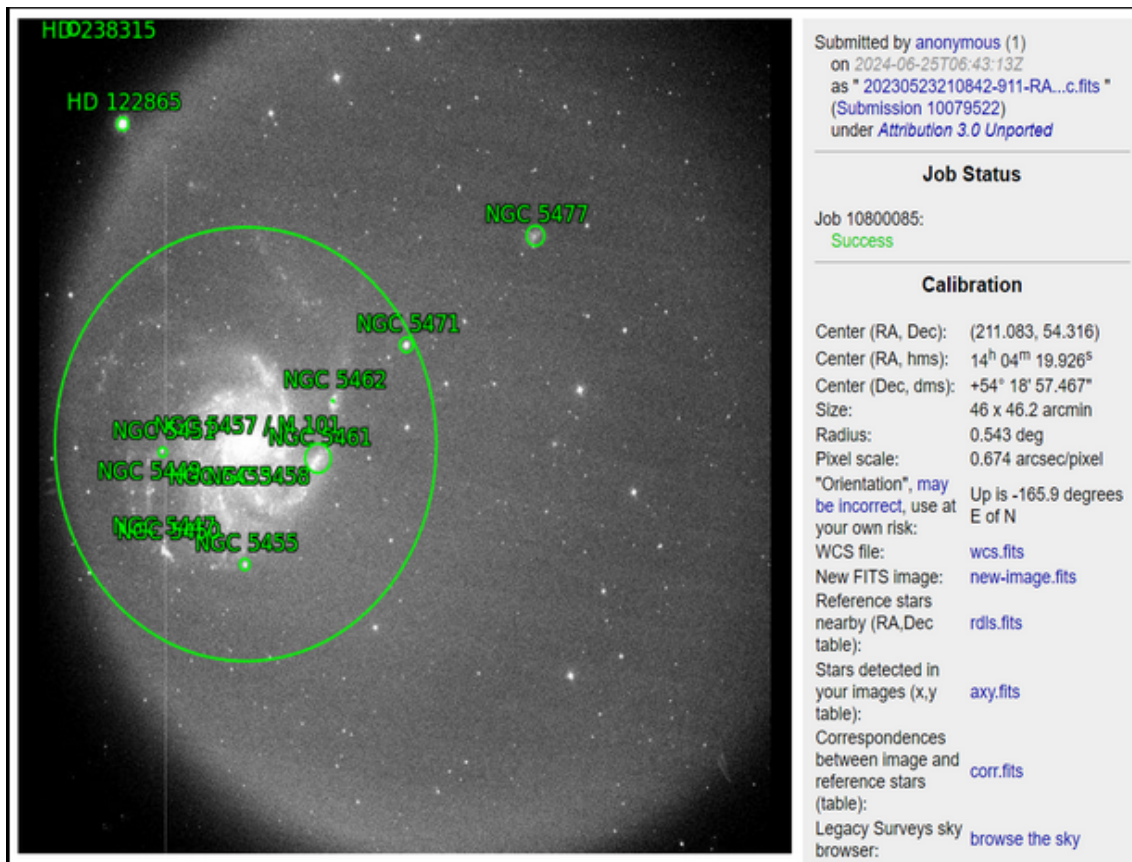
Figure 3.1: Astrometric image taken

# 4. Photometry

## 4.1 Introduction to Photometry

Photometry is the measurement of the flux or intensity of light from celestial objects. It is a fundamental tool in astronomy for determining various properties of stars, such as their brightness, distance, temperature, and size. Photometric data is essential for understanding the physical characteristics of stars and other celestial bodies, including their evolution and composition.(7)

Photometry can be performed in various wavelength bands, ranging from ultraviolet to infrared. The most common photometric system is the Johnson-Cousins UBVRI system, where U (ultraviolet), B (blue), V (visual), R (red), and I (infrared) represent different wavelength filters. The choice of filter depends on the specific objectives of the study and the characteristics of the objects being observed.

## 4.2 Photometry Process

The process of photometry involves the following steps:

1. **Source Detection:** The stars and other celestial objects in the image are identified and their positions are determined. This is typically done using software tools like `SExtractor` (Source Extractor), which detects and catalogs sources in astronomical images.

2. **Aperture Photometry:** The flux from each detected source is measured by summing the pixel values within a specified aperture (a circular region centered on the source). The background flux is subtracted to obtain the net flux.
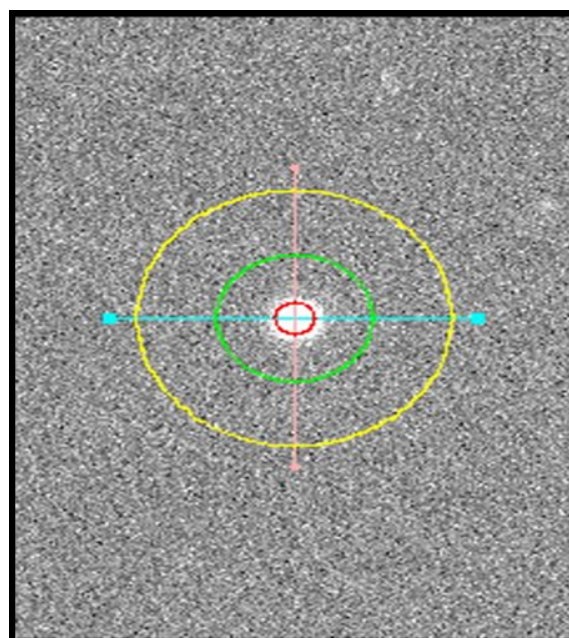


Figure 4.1: Aperture photometry

3. **Point Spread Function (PSF) Photometry:** For crowded fields or faint stars, aperture photometry may not provide accurate results. In such cases, PSF photometry is used, where the light distribution of each star is modeled as a PSF, and the flux is measured by fitting this model to the observed data.
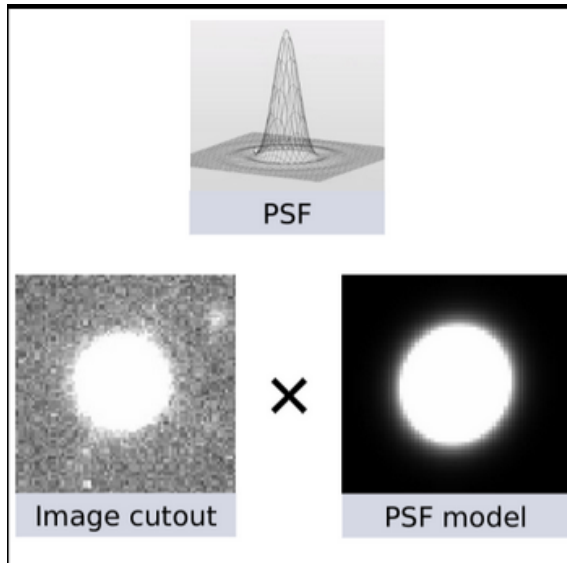
Figure 4.2: Point Source Function

4. **Magnitude Calculation:** The flux is converted into magnitude using the appropriate calibration data. Magnitudes are a logarithmic measure of brightness, where a lower magnitude corresponds to a brighter object.

## 4.3  Photometry for Our Project

In our project, we performed photometry using several external packages to enhance the accuracy of our measurements. We utilized the following tools:

- `Swarp`**(4):** This tool was used for resampling and combining images from different observations. `Swarp` aligns and stacks multiple images to create a final, higher-quality image for analysis.
- `SExtractor`**(3) (Source Extractor):** `SExtractor` was employed to detect and catalog stars in our images. It is particularly effective for identifying bright and isolated stars. However, for faint stars, `SExtractor` does not always provide accurate results due to its reliance on simple aperture photometry.
- `PSFEx`**(2):** For more accurate photometry of faint stars, we used `PSFEx`, which performs PSF photometry. `PSFEx` models the PSF of the image and fits this model to faint stars, allowing us to obtain precise measurements even in crowded fields or for stars near the detection limit.

We began with the use of `SExtractor` to detect and perform photometry on the brighter stars within our field of view. However, due to the limitations of aperture photometry, particularly in cases involving faint stars or crowded fields, we transitioned to PSF photometry using `PSFEx`. This approach enabled us to obtain more reliable photometric measurements, especially for the faint stars that are crucial for our analysis.
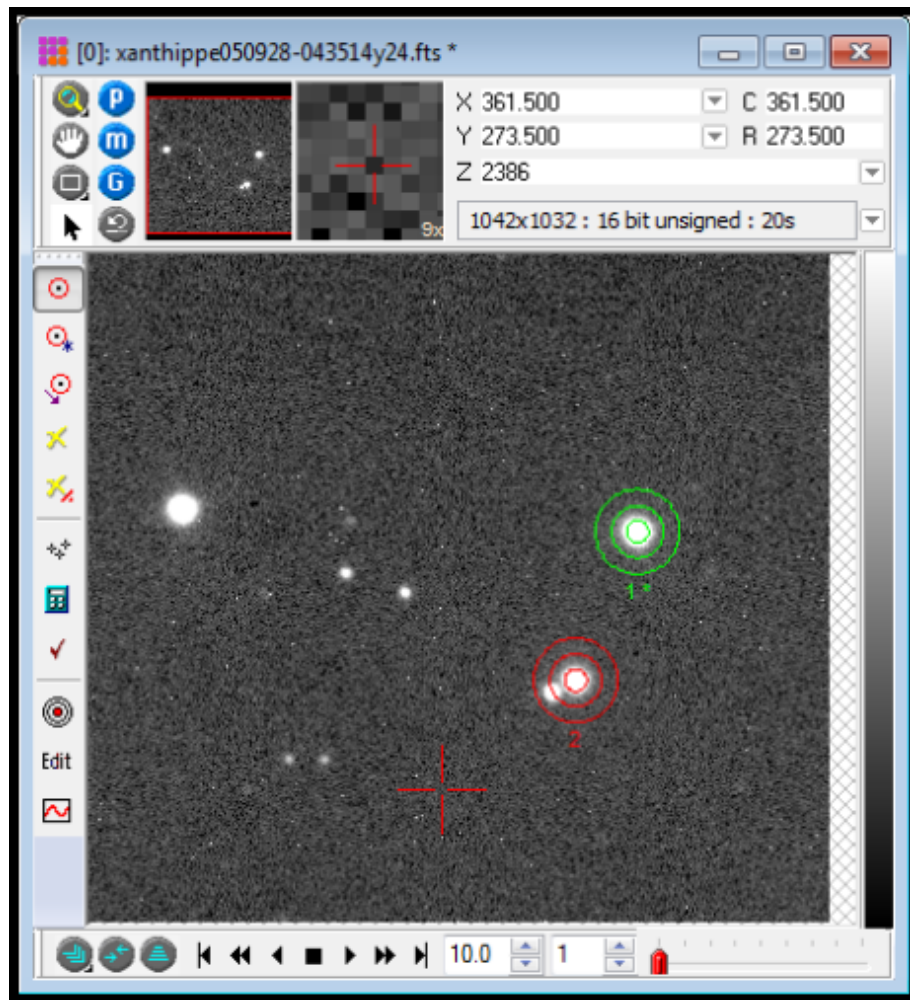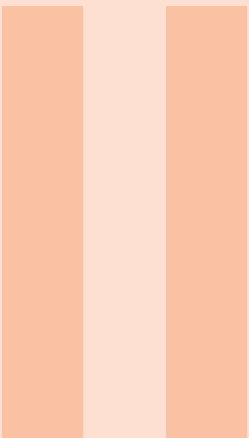
Figure 4.3: Photometric analysis of SN2023ixf using SExtractor and PSFEx.

# Part Two

# 5. PSF Photometry

## 5.1 Point Spread Function (PSF)

The Point Spread Function (PSF) describes how a point source, such as a distant star, appears on a detector due to the effects of the telescope's optics, the atmosphere, and the detector itself. In an ideal scenario, a point source would appear as a single pixel on a detector, but in reality, it is spread over several pixels, resulting in a characteristic distribution of light. This distribution is what we refer to as the PSF.

Mathematically, the PSF can be represented as a function $P(x, y)$, where $x$ and $y$ are the coordinates on the detector plane. The PSF is often modeled using a Gaussian function due to its simplicity and the fact that it closely approximates the distribution of light from a point source(8):

$$P(x, y) = \frac{1}{2\pi\sigma_x\sigma_y} \exp\left(-\frac{1}{2}\left[\left(\frac{x-x_0}{\sigma_x}\right)^2 + \left(\frac{y-y_0}{\sigma_y}\right)^2\right]\right)$$

where:
- $\sigma_x$ and $\sigma_y$ are the standard deviations of the Gaussian in the $x$ and $y$ directions, respectively.
- $(x_0, y_0)$ is the center of the PSF.

In practice, the PSF is determined by observing a star or another point source and measuring how its light is distributed across the detector. The PSF can vary across the field of view due to optical distortions, making it important to model the PSF accurately for different regions of the image.

## 5.2 PSF Photometry

PSF photometry is a technique that utilizes the PSF to measure the flux of stars in an image, particularly in crowded fields where stars are close to each other, or for faint stars where simple aperture photometry may not be accurate. Instead of summing the pixel values within a fixed aperture, PSF photometry fits the PSF model to the observed light distribution of each star, allowing for a more precise measurement of the star's flux.

The basic steps in PSF photometry are as follows:
1. **PSF Modeling:** A PSF model is created by observing a few isolated stars in the image. The parameters of the Gaussian function (or other chosen functions) are adjusted to fit the observed light distribution of these stars.
2. **PSF Fitting:** The PSF model is then fitted to each star in the image. This involves scaling the PSF model to match the brightness of the star and shifting it to align with the star's centroid. The fit is usually performed using a least-squares minimization technique, which adjusts the model parameters to minimize the difference between the observed and modeled light distributions.
3. **Flux Measurement:** The flux of each star is determined from the amplitude of the fitted PSF model. Because the PSF fitting process accounts for overlapping stars and varying backgrounds, the flux measurement obtained from PSF photometry is often more accurate than that from aperture photometry.

## 5.3 PSF Photometry in Our Project

In our project, we performed PSF photometry to accurately measure the flux of SN2023ixf and surrounding stars. The process involved the following steps:

- **PSF Modeling:** We created a PSF model based on isolated stars in the vicinity of SN2023ixf. The PSF was modeled using a Gaussian function, where the parameters were optimized to fit the observed light distribution.
- **PSF Fitting:** The modeled PSF was then fitted to the supernova and other stars in the image. This allowed us to measure the flux of the supernova accurately, even in the presence of nearby stars or background noise.
- **Flux Measurement:** Using the fitted PSF, we extracted the flux values for SN2023ixf. These values were then converted into magnitudes, which are used for further analysis and comparison with theoretical models.

PSF photometry proved to be a crucial tool in our analysis, especially for obtaining reliable measurements in crowded fields or for faint sources. The accuracy of the PSF fitting directly impacted the precision of our photometric measurements. After doing the PSF photometry we have plotted the magnitudes for all bands and plotted against JD.
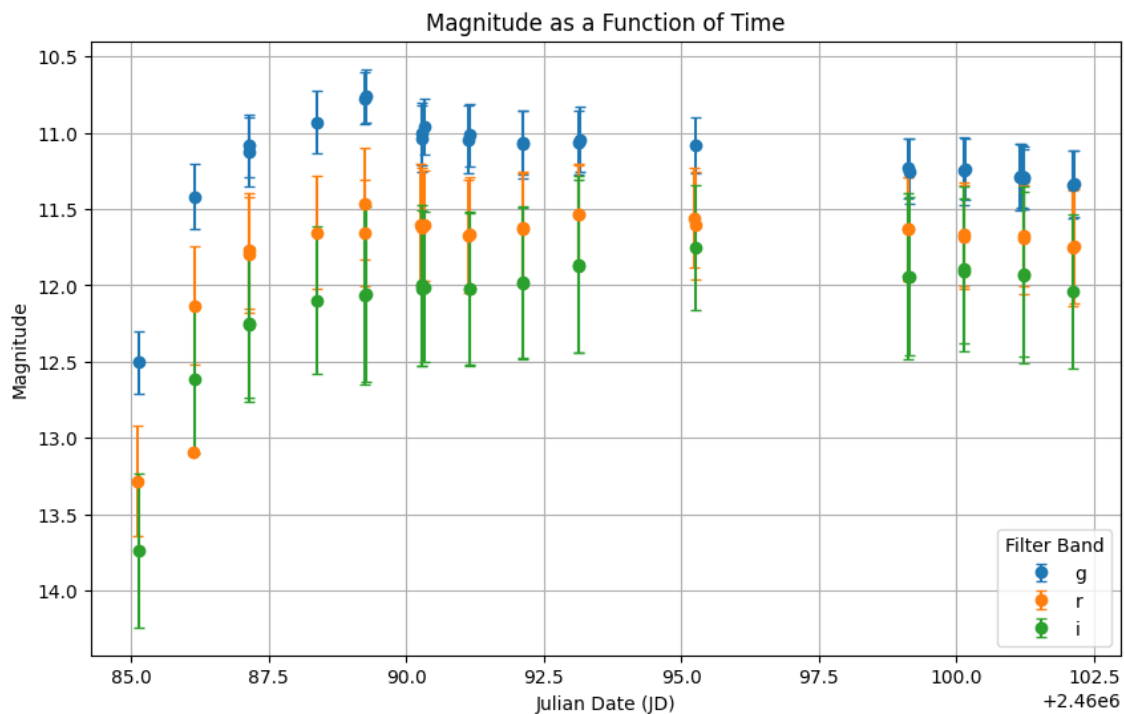


Figure 5.1: PSF fitting process for SN2023ixf and surrounding stars.

# 6. U-Band Phtometry

## 6.1 Introduction to U-band Photometry

Photometry is the science of measuring the flux or intensity of an astronomical object's electromagnetic radiation. U-band photometry specifically refers to measurements made in the ultraviolet (U) portion of the electromagnetic spectrum, typically centered around 365 nm. This band is sensitive to the hot, young stars and is particularly useful in studying star-forming regions, active galactic nuclei, and the early stages of supernovae.(10)

The U-band is more challenging than other optical bands due to its sensitivity to atmospheric extinction and the lower quantum efficiency of detectors at shorter wavelengths. Despite these challenges, U-band observations are invaluable in astrophysical research, offering insights into the temperature, metallicity, and age of stellar populations.

## 6.2 Photometric Analysis of SN2023ixf in the U-band

**Point Spread Function (PSF) Fitting** Given the crowded field and the need for precise flux measurements, the Point Spread Function (PSF) fitting method was employed. PSF fitting models the shape of the stellar profile in the image, allowing for accurate flux determination even in the presence of overlapping sources or varying background noise. The steps involved in this process are as follows:

1. **PSF Generation:** The PSF for each U-band image was generated using the PSFEx software. SExtractor was first used to extract sources and measure their initial properties. PSFEx then constructed a PSF model by analyzing bright, isolated stars in the field.
2. **PSF Normalization:** The PSF model was normalized to ensure that the total flux within the PSF aperture matched the flux expected for a point source.
3. **Flux Measurement:** The normalized PSF model was then used to fit the observed profile of SN2023ixf and the reference stars. This process accounted for the background noise and instrumental effects, providing accurate flux measurements.

## 6.3 Calculation of Instrumental Magnitudes

The instrumental magnitudes were calculated using the flux values obtained from the PSF fitting process. The conversion from flux to magnitude was performed using the following relation:

$$m_{\text{inst}} = -2.5 \log_{10}\left(\frac{F}{t_{\exp}}\right) + C \tag{6.1}$$

where $F$ is the measured flux, $t_{\exp}$ is the exposure time, and $C$ is a constant that depends on the specific detector characteristics.

The instrumental magnitudes for SN2023ixf and the six reference stars were computed for each U-band image.

## 6.4 Zero-Point Calibration

To convert the instrumental magnitudes to a standard magnitude system, a zero-point (ZP) calibration was performed using the reference stars with known magni-

tudes from the SDSS catalog(12). The calibration process involved the following steps:

1. **Calculate Offsets:** The difference between the instrumental magnitudes and the catalog magnitudes for each reference star was computed for each image.
2. **Determine Zero-Point:** The median of these offsets was taken as the zero-point for each image.
3. **Apply Zero-Point:** The calculated zero-point was then added to the instrumental magnitudes of SN2023ixf, resulting in calibrated magnitudes.
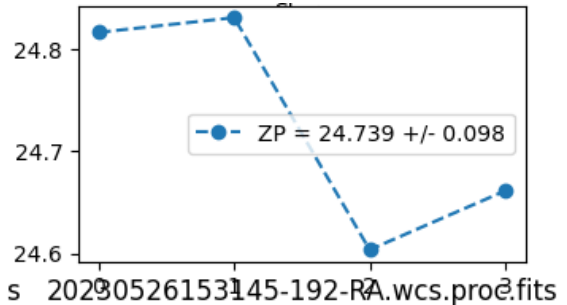


Figure 6.1: Zero point estimation

The zero-point errors were estimated from the standard deviation of the offsets among the reference stars. The calibrated magnitudes provided a reliable measure of the U-band flux of SN2023ixf, enabling a detailed analysis of its light curve evolution.

The calibrated U-band magnitudes of SN2023ixf were successfully obtained, showing the temporal evolution of its light curve. The analysis demonstrated the utility of PSF fitting in accurately measuring the flux in crowded fields and the importance of zero-point calibration in achieving reliable photometric results.

The variation in the zero-point across different images was minimal, indicating consistent photometric conditions and accurate calibration.

The U-band photometric analysis of SN2023ixf using PSF fitting and zero-point calibration provided essential data for understanding the supernova's behavior. This methodology can be extended to other bands and epochs, offering a comprehensive picture of SN2023ixf's evolution. After doing the U-band photometry again we plotted the magnitudes against JD and combined with all the data we have
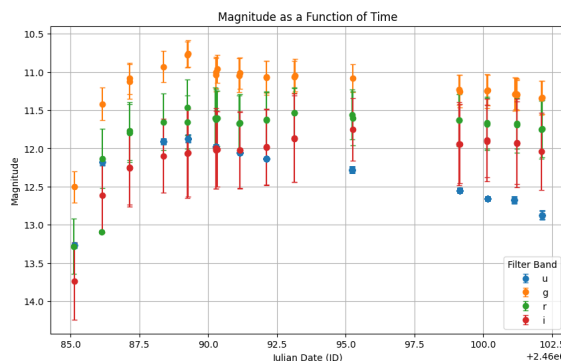


Figure 6.2: The combined magnitudes of all filters

# 7. Model fitting

## 7.1 Introduction to Supernova Modeling

Modeling a supernova involves understanding the physical processes that govern its explosion and subsequent evolution. The key objective is to estimate parameters such as the mass of Nickel-56 ($^{56}$Ni), ejecta mass, explosion energy, and other physical properties that provide insight into the progenitor star and the nature of the explosion.

For this study, we used the `SuperBol` package, which allows for the estimation of blackbody-corrected luminosity, temperature evolution, and radius change as a function of time. However, our approach relies primarily on a simplified luminosity model, which limits the accuracy of our estimates. To obtain more accurate results, additional hydrodynamical modeling would be required.

## 7.2 Estimating Nickel Mass and Characteristic Time

The mass of $^{56}$Ni produced in the explosion is a crucial parameter, as it influences the light curve and peak luminosity of the supernova. To estimate the Nickel mass, we used the following luminosity model from the literature[14]:

$$L(t) = L_0 \cdot M_{\text{Ni}} \cdot \left[ \exp\left( \frac{-\Delta t}{t_{\text{Co}}} \right) - \exp\left( \frac{-\Delta t}{t_{\text{Ni}}} \right) \right] \cdot \left[ 1 - \exp\left( \frac{-t_c^2}{\Delta t^2} \right) \right] \tag{7.1}$$

where:
- $L(t)$ is the luminosity at time $t$,
- $L_0$ is the initial luminosity at the start of the explosion,
- $M_{\text{Ni}}$ is the mass of $^{56}$Ni,
- $t_{\text{Co}}$ and $t_{\text{Ni}}$ are the decay timescales of Cobalt and Nickel, respectively,
- $\Delta t$ is the time since explosion,
- $t_c$ is the characteristic time.

By fitting this model to the observed light curve, we determined the Nickel mass and the characteristic time of the supernova.
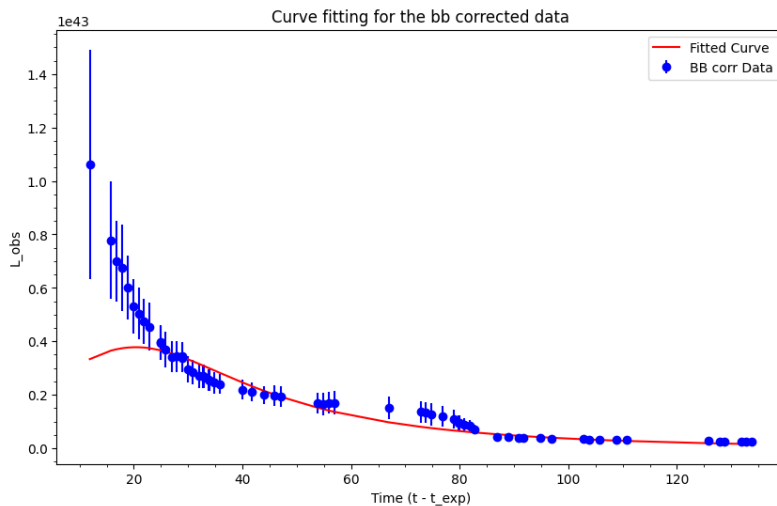


Figure 7.1: Model fitting

The estimated mass of Nickel fro our model fitting was around $0.0637 \pm 0.0006 M_\odot$ and the Charechteristic time was $187.05 \pm 5.05 \text{sec}$

## 7.3 Ejecta Mass and Explosion Energy

The ejecta mass ($M_{ej}$) and explosion energy ($E_{exp}$) are critical parameters that provide insight into the progenitor star's properties. The ejecta mass represents the total mass of material ejected during the explosion, while the explosion energy is the kinetic energy imparted to the ejecta(14).

We used the following equations to estimate these parameters:

$$\log E_{51} = -0.728 + 2.148 \log L_{42} - 0.280 \log M_{Ni} + 2.091 \log t_{p2} - 1.632 \log R_{500} \qquad (7.2)$$

$$\log M_{10} = -0.947 + 1.474 \log L_{42} - 0.518 \log M_{Ni} + 3.867 \log t_{p2} - 1.120 \log R_{500} \qquad (7.3)$$

where:

- $E_{51}$ is the explosion energy in units of $10^{51}$ ergs,
- $M_{10}$ is the ejecta mass in units of $10 M_{\odot}$,
- $L_{42}$ is the peak luminosity in units of $10^{42}$ ergs/s,
- $t_{p2}$ is the peak time in units of $10^{2}$ days,
- $R_{500}$ is the radius of the progenitor in units of $500 R_{\odot}$.
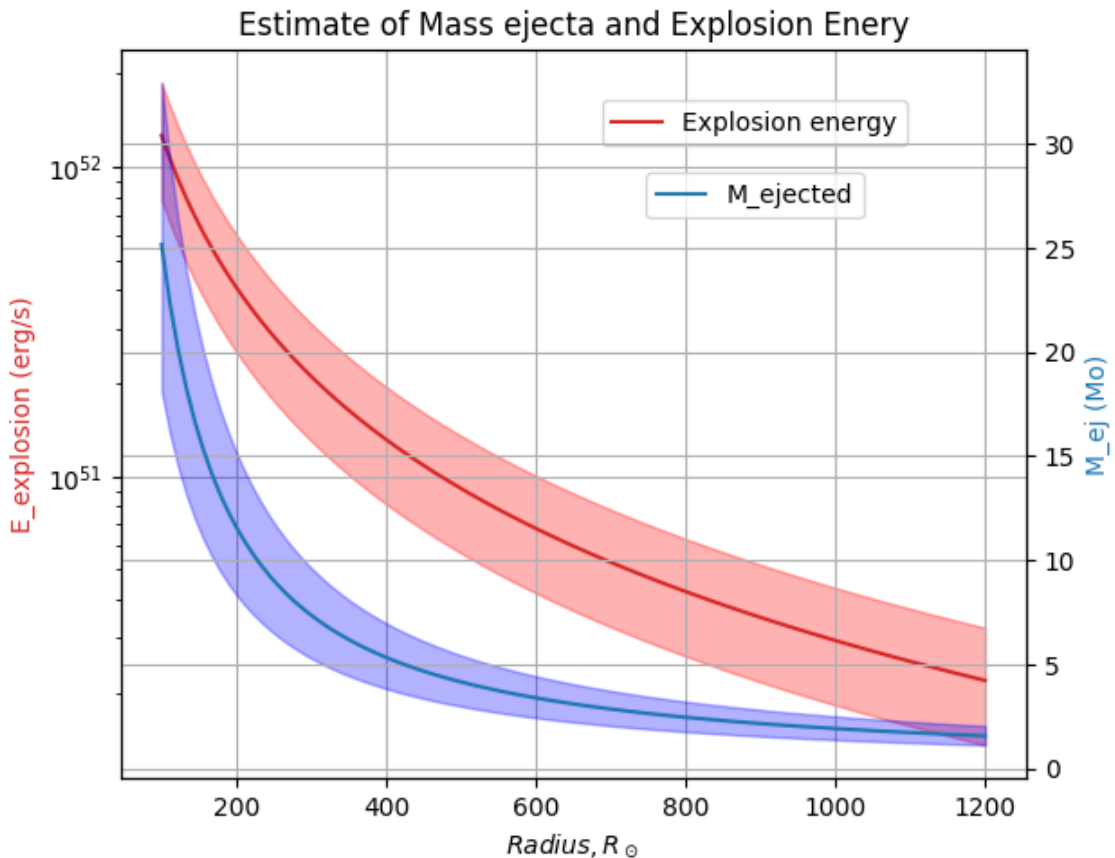


Figure 7.2: The estimation of Mass ejecta and Explosion energy

These parameters help us infer the nature of the progenitor star and the dynamics of the explosion. By analyzing the ejecta mass and explosion energy, we can

estimate whether the progenitor was a massive star and gain insights into the mechanisms driving the explosion.

The modeling of SN2023ixf provided estimates of key parameters such as the $^{56}$Ni mass, ejecta mass, and explosion energy. While the results offer valuable insights, the limitations of using a purely luminosity-based model should be acknowledged. Future work could involve more sophisticated hydrodynamical modeling to improve the accuracy of these estimates and better understand the progenitor system of this supernova.

## 7.4  Assumptions and Limitations

In this modeling, we assume that the luminosity of the supernova can be described by the decay of radioactive isotopes, particularly $^{56}$Ni, which decays into Cobalt-56 ($^{56}$Co) and then into Iron-56 ($^{56}$Fe). This approach assumes a spherically symmetric explosion with homogeneous ejecta, which may not always be the case in real supernovae.

Since we only used the luminosity model, the results may not fully capture the complexities of the explosion dynamics. Accurate modeling would require solving the full set of hydrodynamical equations governing the explosion, considering factors such as asymmetry, clumping in the ejecta, and interaction with the circumstellar medium (CSM).

# 8. Conclusion

## 8.1 Summary of Findings

The study of SN2023ixf has significantly enhanced our understanding of Type II supernovae, particularly regarding explosion mechanics and progenitor characteristics. Utilizing observational data, we have estimated essential parameters such as the mass of Nickel-56 produced, the total ejecta mass, and the explosion energy. Despite relying on a luminosity-based model, these estimates offer valuable insights into the supernova's underlying processes.

## 8.2 Limitations of the Current Model

While the modeling of SN2023ixf provides useful insights, it also reveals the limitations of relying solely on luminosity data. Supernovae are complex phenomena with intrinsic asymmetries, ejecta clumping, and interactions with the circumstellar medium that simplified models may not fully address. These factors underscore the need for more sophisticated approaches, such as hydrodynamical modeling, to better capture the physical processes involved.

## 8.3 Assumptions and Future Directions

The study's assumptions, including spherical symmetry and homogeneous ejecta, are standard in many initial analyses but may not fully represent the actual explosion conditions. Future research should integrate advanced computational models and multi-wavelength observations to refine our understanding of supernovae like SN2023ixf. This approach will improve parameter accuracy and provide deeper insights into progenitor systems and explosion dynamics.

## 8.4 Concluding Remarks

This study marks a significant step in the investigation of SN2023ixf and contributes to the broader field of supernova research. Although preliminary, these findings lay the foundation for future studies that aim to uncover the remaining mysteries of similar supernovae. Ongoing advancements in observational techniques and theoretical models will enhance our understanding of stellar evolution and the dynamic processes shaping our universe.

## 8.5 Software and Packages Used

This project utilized several software packages and tools for data analysis and processing:
**NumPy**(6),**SciPy** (16),**Matplotlib** (9),**Swarp**(4),**SExtractor** (3),**PSFEx** (2),**photutils** (0),**Aperture Photometry Tool** (11),**SuperBol** (0)

## 8.6 Code available on:

`https://github.com/GAURAVBHOIR/KSP5.0_study-of-sn2023ixf`

(Ber88)   Sidney van den Bergh. "Classification of supernovae and their remnants". In: *Astrophysical Journal, Part 1 (ISSN 0004-637X), vol. 327, April 1, 1988, p. 156-163.* 327 (1988), pages 156–163 (cited on page 6).

(Ber11)   E. Bertin. "Automated Morphometry with SExtractor and PSFEx". In: A&AS. Astronomical Society of the Pacific Conference Series 442 (July 2011). Edited by I. N. Evans et al., page 435 (cited on pages 22, 36).

(BA96)    E. Bertin and S. Arnouts. "SExtractor: Software for source extraction." In: A&AS 117 (June 1996), pages 393–404. DOI: 10.1051/aas:1996164 (cited on pages 22, 36).

(Ber+02)  Emmanuel Bertin et al. "The TERAPIX Pipeline". In: A&AS. Astronomical Society of the Pacific Conference Series 281 (Jan. 2002). Edited by David A. Bohlender, Daniel Durand, and Thomas H. Handley, page 228 (cited on pages 22, 36).

(Far+14)  T Faran et al. "A sample of Type II-L supernovae". In: *Monthly Notices of the Royal Astronomical Society* 445.1 (2014), pages 554–569 (cited on page 7).

(Har+20)  Charles R. Harris et al. "Array programming with NumPy". In: *Nature* 585.7825 (Sept. 2020), pages 357–362. DOI: 10.1038/s41586-020-2649-2. URL: https://doi.org/10.1038/s41586-020-2649-2 (cited on page 36).

(HK82)    Arne A Henden and Ronald H Kaitchuck. "Astronomical photometry". In: *New York: Van Nostrand Reinhold* (1982) (cited on page 21).

(How89)   Steve B Howell. "Two-dimensional aperture photometry: signal-to-noise ratio of point-source observations and optimal data-extraction techniques". In: *Publications of the Astronomical Society of the Pacific* 101.640 (1989), page 616 (cited on page 26).

(Hun07)   J. D. Hunter. "Matplotlib: A 2D graphics environment". In: *Computing in Science & Engineering* 9.3 (2007), pages 90–95. DOI: 10.1109/MCSE.2007.55 (cited on page 36).

(Ira+24)  Ido Irani et al. "The Early Ultraviolet Light Curves of Type II Supernovae and the Radii of Their Progenitor Stars". In: *The Astrophysical Journal* 970.1 (2024), page 96 (cited on page 29).

(Jos+12)  Robert G. Joseph et al. "Aperture Photometry Tool". In: *Publications of the Astronomical Society of the Pacific* 124.917 (July 2012), page 737. DOI: 10.1086/666883 (cited on page 36).

(MB15)    Andrew W Mann and Kaspar von Braun. "Revised filter profiles and zero points for broadband photometry". In: *Publications of the Astronomical Society of the Pacific* 127.948 (2015), page 102 (cited on page 30).

(Pan+23)  Sonja Panjkov et al. "Probing the soft X-ray properties and multi-wavelength variability of SN2023ixf and its progenitor". In: *arXiv preprint arXiv:2308.13101* (2023) (cited on page 8).

(Sin+24)  Avinash Singh et al. "Unravelling the asphericities in the explosion and multi-faceted circumstellar matter of SN 2023ixf". In: *arXiv preprint arXiv:2405.20989* (2024) (cited on pages 32, 33).

(Tej+23)    Rishabh Singh Teja et al. "Far-ultraviolet to near-infrared observations of SN 2023ixf: a high-energy explosion engulfed in complex circumstellar material". In: *The Astrophysical Journal Letters* 954.1 (2023), page L12. DOI: `https://doi.org/10.3847/2041-8213/acef20` (cited on page 9).

(Vir+20)    Pauli Virtanen et al. "SciPy 1.0: Fundamental Algorithms for Scientific Computing in Python". In: *Nature Methods* 17 (2020), pages 261–272. DOI: `10.1038/s41592-019-0686-2` (cited on page 36).

(Zap+19)    Emmanouil Zapartas et al. "The diverse lives of progenitors of hydrogen-rich core-collapse supernovae: the role of binary interaction". In: *Astronomy & Astrophysics* 631 (2019), A5 (cited on page 8).